

# Rhizaria in the oligotrophic ocean exhibit clear temporal and vertical variability.

Alex Barth<sup>\*1</sup>, Leocadio Blanco-Berical<sup>2</sup>, Rod Johnson<sup>2</sup>  
and Joshua Stone<sup>1</sup>

1. University of South Carolina, Biological Sciences, 700 Sumter St  
401, Columbia, SC 29208
2. Arizone State University, School of Ocean Futures, Bermuda  
Institute of Ocean Sciences 17 Biological Station, St Georges,  
GE 01

## Abstract

Recently studies have shown that Rhizaria, a super-group of marine protists have a large role in pelagic ecosystems. They are unique in that they construct mineral tests out of silica, calcium carbonate, or strontium sulfate. As a consequence, Rhizaria can have large impacts on the ocean's cycling of carbon and other elements. However, less is known about Rhizarian ecology or their role in the pelagic food-web. Some taxa, like certain Radiolarians are mixotrophic, hosting algal symbionts. While other taxa are flux-feeders or even predatory carnivores. Some prior research has suggested that Rhizaria will partition vertically in the water column, likely due to different trophic strategies. However, very few studies have investigated their populations over extended periods of time. In this study, we present data investigating Rhizarian abundance and vertical distribution from over a year of monthly cruises into the Sargasso Sea. This study represents the first quantification of Rhizaria throughout the mesopelagic zone in an oligotrophic system for an extended period of time. We use this data to investigate the hypothesis that Rhizaria taxonomic groups will partition due to trophic mode. We also investigate how their abundance varies in accordance with a variety of environmental parameters. Rhizaria abundance was quantified using an Underwater Vision Profiler (UVP5), an in-situ imaging device. Ultimately, we show that different Rhizaria taxa will have unique vertical distribution patterns. Models relating their abundance to environmental parameters have mixed results, yet particle concentration is a common predictive variable, supporting the importance of heterotrophy amongst many taxa.

## **2      Introduction**

**3** Rhizaria are an extremely diverse super-group of single-celled organisms consist-  
**4** ing of several phyla including Retaria (foraminifera and radiolaria) and Cercozoa.  
**5** These organisms exist in a wide range of habitats and are widely represented  
**6** in plankton communities throughout the global ocean. While the taxonomy of  
**7** these organisms has recently undergone several reclassifications (Biard, 2022a),  
**8** their presence in ocean ecosystems has been long known to oceanographers.  
**9** Some of the earliest records of their existence are from oceanographic expedi-  
**10** tions in the 19th century (Haekel, 1887). Rhizaria are unique members of the  
**11** plankton and protist community because they can reach large sizes (up to sev-  
**12** eral mm in diameter) and they construct intricate mineral skeletons out of either  
**13** silica, strontium, or calcium carbonate (Biard, 2022a; Kimoto, 2015; Nakamura  
**14** and Suzuki, 2015; Suzuki and Not, 2015). Despite their noticeable morphology  
**15** and global distribution, Rhizaria were largely understudied throughout the 20th  
**16** century. The bulk of modern plankton research has focused on hard-bodied crus-  
**17** tacea which are numerically dominant and easily sampled with nets and preser-  
**18** vatives. Fragile organisms like Rhizaria, were difficult to adequately study as  
**19** they can be destroyed through standard zooplankton sampling techniques and  
**20** preserve poorly. A number of studies in the late 1900s did employ alternative  
**21** techniques to quantify Rhizaria including diaphragm pumps (Michaels, 1988) or  
**22** blue-water SCUBA collections (Bijma et al., 1990; Caron et al., 1995; Caron and  
**23** Be, 1984). However, the bulk of Rhizaria research was constrained to sediment  
**24** traps or paleontological studies of sediment (Boltovskoy et al., 1993; Takahashi

<sup>25</sup> et al., 1983). Only recently has the advent of molecular techniques and in-situ  
<sup>26</sup> imaging tools ignited a renewed focus on Rhizaria in pelagic ecosystems (Caron,  
<sup>27</sup> 2016).

<sup>28</sup> The wave of new data on Rhizaria has facilitated an improved understanding of  
<sup>29</sup> the significance in ocean ecosystem functions. Firstly, taxonomists have been  
<sup>30</sup> able to greatly refine the understanding of evolutionary relationships amongst  
<sup>31</sup> these diverse protists (Aurahs et al., 2009; Biard et al., 2015; Cavalier-Smith et  
<sup>32</sup> al., 2018; Decelle et al., 2013, 2012; rev by Biard, 2022a). DNA metabarcoding  
<sup>33</sup> studies have revealed insights into the distributional patterns Llopis Monferrer  
<sup>34</sup> et al. (2022), ecological relationships (Decelle et al., 2012; Nakamura et al.,  
<sup>35</sup> 2023), and contribution to biogeochemical fluxes (Guidi et al., 2016; Gutierrez-  
<sup>36</sup> Rodriguez et al., 2019). Transcriptomic and proteomic approaches also have  
<sup>37</sup> been used to quantify rhizarian contribution to community metabolism (Cohen  
<sup>38</sup> et al., 2023). Yet, despite the excellent taxonomic resolution provided by molec-  
<sup>39</sup> ular approaches, they do not provide a truly quantitative metric for estimating  
<sup>40</sup> Rhizarian abundance or biomass. In-situ imaging tools however, offer the ability  
<sup>41</sup> to observe organisms in the natural state and quantify their abundance (Barth  
<sup>42</sup> and Stone, in review; Ohman, 2019). While there were early applicaitons of  
<sup>43</sup> imaging tools to document Rhizaria (Dennett et al., 2002), Biard et al. (2016)'s  
<sup>44</sup> report from a global imaging dataset highlighted the importance of Rhizaria to  
<sup>45</sup> the total standing stock of marine carbon. Due to their large sizes, ability to  
<sup>46</sup> concentrate smaller particles and the unique structure of their mineral skeletons,  
<sup>47</sup> Rhizaria have the potential to massively influence ocean biogeochemical cycling.

48 A number of studies have made large advances in estimating the contribution  
49 of Rhizaria to ocean cycling of carbon (Gutierrez-Rodriguez et al., 2019; Ike-  
50 noue et al., 2019; Lampitt et al., 2009; Stukel et al., 2018), silica (Biard et al.,  
51 2018; Llopis Monferrer et al., 2021), and strontium (Decelle et al., 2013). Still,  
52 Rhizarian ecological roles are not well understood (Biard, 2022a). This is a  
53 major challenge as it is critical to understand the ecological role of plankton to  
54 fully incorporate them into biological oceanographic models.

55 The ecological role of Rhizaria in plankton communities is complicated due to  
56 the fact different taxa can exhibit every different trophic modes. As zooplank-  
57 ton, rhizaria are predominately heterotrophic (Biard, 2022a), yet their feeding  
58 modes can be quite varied. Phaeodarians (family Cercozoa) are largely thought  
59 to be flux-feeders, collecting and feeding on sinking particles (Nakamura and  
60 Suzuki, 2015; Stukel et al., 2019). Alternatively, Retaria can be either exclu-  
61 sively heterotrophic or mixotrophic, utilizing photosynthetic algal symbionts  
62 (Anderson, 2014; Decelle et al., 2015). Mixotrophic foraminifera host a variety  
63 of endosymbiont partners (Decelle et al., 2015; Lee, 2006), which are thought to  
64 support early and adult life stages and contribute to total primary productivity  
65 (Kimoto, 2015). Still, foraminifera are omnivorous, possibly even predominately  
66 carnivorous with several studies suggesting that they can be effective predators  
67 (Anderson and Bé, 1976; Gaskell et al., 2019), mainly consuming live copepods  
68 (Caron and Be, 1984). Radiolaria have several lineages all which have some taxa  
69 who are well known to host symbionts (Biard, 2022b). Amongst radiolarians, ar-  
70 guably the most widespread are Collodaria who can be either large solitary cells

71 or form massive colonies, up to several meters in length (Swanberg and Ander-  
72 son, 1981). All known Collodaria species host dinoflagellate symbionts (Biard,  
73 2022b) and can contribute substantially to primary productivity, particularly  
74 in oligotrophic ocean regions (Caron et al., 1995; Dennett et al., 2002). This  
75 Collodaria-symbiont association has been suggested as a reason for their high  
76 abundances throughout the photic zone of oligotrophic environments globally  
77 (Biard et al., 2017, 2016). A few Acantharean (Radiolarian order) clades host  
78 algal symbionts (Biard, 2022b; Decelle et al., 2012), notably with two clades  
79 forming an exclusive relationship with Phaeocystis. However, globally Acan-  
80 tharea are less abundant than Collodaria (Biard, 2022a) and contribute less to  
81 total primary productivity (Michaels et al., 1995). This may be due to the fact  
82 several clades of Acantharea are cyst-forming and strictly heterotrophs (Biard,  
83 2022b; Decelle et al., 2013). Furthermore, Mars Brisbin et al. (2020) docu-  
84 mented apparent predation behavior in Acantharea near the surface, suggesting  
85 that there may be a large reliance on carnivory.

86 Given the high abundances, yet diverse trophic strategies found among Rhizar-  
87 ian taxa, it is reasonable to expect some form of niche partitioning. A number  
88 of studies do suggest evidence for vertical zonation between Rhizaria groups  
89 according to various trophic strategies. Taxa-specific studies of radiolarians sug-  
90 gest they may be restricted to the euphotic zone (Boltovskoy, 2017; Michaels,  
91 1988). Although some studies report Acantharea in deeper waters (Decelle et  
92 al., 2013; Gutiérrez-Rodríguez et al., 2022). Phaeodarians alternatively, are  
93 generally found in the mesopelagic where photosynthesis cannot occur but they

94 can feed on sinking particles (Stukel et al., 2018). In an imaging-based study of  
95 the whole Rhizaria community, Biard and Ohman (2020) noted clear patterns  
96 in vertical zonation which largely corresponded to different trophic roles. In  
97 the oligotrophic ocean, Blanco-Bercial et al. (2022) also noted that the protist  
98 community, including Rhizaria, partition along an autotroph and mixotroph to  
99 heterotroph gradient with increasing depth in the water column. Yet, few stud-  
100 ies have made direct attempts to relate rhizaria abundances to environmental  
101 factors (Biard and Ohman, 2020). In part, this is due to the fact few stud-  
102 ies have been able to sample Rhizaria in the same location over a consistent  
103 timeframe (Boltovskoy et al., 1993; Gutiérrez-Rodríguez et al., 2022; Hull et  
104 al., 2011; Michaels et al., 1995; Michaels, 1988). Furthermore, no studies have  
105 utilized imaging, arguably the best method for quantifying rhizaria, consistently  
106 throughout the full mesopelagic. Given this lack of information, there are many  
107 unknowns with respect to Rhizarian ecology, seasonality and phenology across  
108 different groups.

109 In this study, we present a comprehensive assessment of large Rhizaria measured  
110 for multiple months (greater than 1 year) using an in-situ imaging approach.  
111 With this dataset, we address two critical aims. 1) Quantification of large  
112 Rhizaria throughout the epipelagic (0-200m) and mesopelagic (200-1000m) over  
113 the course of an annual cycle. These data were collected in the Sargasso Sea,  
114 and represents the first study of its kind in an oligotrophic system. 2) We aim to  
115 test the hypothesis that Rhizaria exhibit niche partitioning according to trophic  
116 roles. This hypothesis makes several predictions, including vertical zonation, as

<sup>117</sup> seen in prior studies, but also that environmental variables related to trophic  
<sup>118</sup> strategy will explain abundance patterns. Specifically, autotrophic/mixotrophic  
<sup>119</sup> taxa will correspond to variables related to autotrophy (chl-a concentration,  
<sup>120</sup> primary productivity, high  $O_2$ ) and other rhizaria will correspond to factors  
<sup>121</sup> which promote heterotrophy (particle concentration, flux, and low  $O_2$ ).

## <sup>122</sup> Methods

### <sup>123</sup> Oceanographic Sampling

<sup>124</sup> Data were collected in collaboration with the Bermuda Atlantic Time-Series  
<sup>125</sup> Study (Lomas et al., 2013; Michaels and Knap, 1996) on board the R/V  
<sup>126</sup> Atlantic Explorer. Cruises were conducted at approximately monthly intervals.  
<sup>127</sup> Rhizaria individuals were sampled using the Underwater Vision Profiler 5  
<sup>128</sup> [UVP5; Picheral et al. (2010)], a tool which is well established to accurately  
<sup>129</sup> quantify large Rhizaria (Barth and Stone, 2022; Biard et al., 2016; Biard and  
<sup>130</sup> Ohman, 2020; Drago et al., 2022; Llopis Monferrer et al., 2022; Panaiotis et  
<sup>131</sup> al., 2023; Stukel et al., 2019; Stukel et al., 2018). The UVP5 was mounted  
<sup>132</sup> to the sampling rosette and collected data autonomously on routine casts,  
<sup>133</sup> from which only the downcast data are utilized. The UVP5 was deployed  
<sup>134</sup> from June-September 2019 then from October 2020 - January 2022. Casts  
<sup>135</sup> were filtered to only include data collected in the BATS region, far offshore  
<sup>136</sup> of Bermuda into the Sargasso Sea (approximately  $31.0^\circ N$ - $32.5^\circ N$ ,  $64.25^\circ W$ -  
<sup>137</sup>  $63^\circ W$ ; Supplemental Figure 1). In general, casts extended to either 200m,

<sup>138</sup> 500m, or 1200m deep, with a few extended into the bathypelagic (4500m).

<sup>139</sup> However, Rhizaria were only typically found in large abundances throughout  
<sup>140</sup> the epipelagic and mesopelagic zones. As such, we limit this study to results  
<sup>141</sup> from the upper 1000m of the water column.

<sup>142</sup> A variety of biotic and abiotic data were collected during each BATS cruise.

<sup>143</sup> Briefly, we will explain the data utilized in this study. The UVP5 provided  
<sup>144</sup> particle count data at a high-frequency from each cast. Particle concentra-  
<sup>145</sup> tion was calculated from this data for all particles  $184\mu m - 450\mu m$ . The lower  
<sup>146</sup> size range was set by what could be reliably sampled by the UVP5's pixel res-  
<sup>147</sup> olution ( $>2px$ ) and the upper size range is representative of a potential prey  
<sup>148</sup> field for mesozooplankton (Whitmore and Ohman, 2021). Salinity, temperature,  
<sup>149</sup> Dissolved Oxygen (DO), and in-situ chlorophyll fluorescence were measured at  
<sup>150</sup> high-frequencies on each cast, attached to the same CTD rosette as the UVP. On  
<sup>151</sup> certain casts, niskin bottles were used to collect bacterial abundance estimates  
<sup>152</sup> (via epifluorescence microscopy) as well as measure inorganic nutrients ( $NO_3$ ,  
<sup>153</sup> and  $Si$  as silicate/silic acid) at discrete depths. On each cruise, flux estimates  
<sup>154</sup> of total mass, carbon, and nitrogen were also collected using sediment traps (in  
<sup>155</sup> the present study we utilize flux to the mesopelagic as the flux at 200m). Also  
<sup>156</sup> primary productivity was estimated through measuring  $C^{14}$  uptake rates from  
<sup>157</sup> in-situ incubations. Full descriptions of the BATS sampling program, methods,  
<sup>158</sup> and data are available freely online (<https://bats.bios.asu.edu/bats-data/>) and  
<sup>159</sup> reviewed in (Lomas et al., 2013).

<sup>160</sup> Environmental data were processed in a variety of ways to match the format

<sup>161</sup> of the Rhizaria abundance estimates (See below). CTD data were collected at  
<sup>162</sup> higher frequency than the UVP, so these data were averaged within matching  
<sup>163</sup> bins to the UVP5 data. Data from niskin bottles were first linearly interpolated  
<sup>164</sup> with a 1m resolution for each cast where data were available. Then, because data  
<sup>165</sup> were collected at different frequencies over the course of a cruise, the interpo-  
<sup>166</sup> lated data were averaged across casts, then averaged into matching UVP5-sized  
<sup>167</sup> bins. Primary productivity estimates were totaled within the euphotic zone to  
<sup>168</sup> represent a “total euphotic productivity”. Finally the data from the sediment  
<sup>169</sup> trap deployed to 200m was used to represent “flux to the mesopelagic”.

## <sup>170</sup> Rhizaria imaging processing and quantification

<sup>171</sup> Individual vignettes of Rhizaria images were identified using the classification  
<sup>172</sup> platform Ecotaxa (Picheral et al., n.d.). Data were pre-sorted utilizing a  
<sup>173</sup> random-forest classifier and pre-trained learning set. Taxonomic classifica-  
<sup>174</sup> tion were done based on morphology exclusively. While there are sparse  
<sup>175</sup> taxonomic guides for in-situ images of rhizaria, identification largely relied  
<sup>176</sup> on descriptions in (Nakamura and Suzuki, 2015; Suzuki and Not, 2015; and  
<sup>177</sup> Biard and Ohman, 2020). Using the aforementioned sources and publicly  
<sup>178</sup> available ecotaxa projects, I constructed a guide which can be found here:  
<sup>179</sup> [https://thealexbarth.github.io/media//Project\\_Items/Oligotrophic\\_Communi-](https://thealexbarth.github.io/media//Project_Items/Oligotrophic_Communi-)  
<sup>180</sup> [ecotaxa\\_UVP-guide-stone-lab.pdf](https://thealexbarth.github.io/media//Project_Items/Oligotrophic_Community/ecotaxa_UVP-guide-stone-lab.pdf). Broadly, Rhizaria were classified  
<sup>181</sup> as Foraminifera, Radiolarians (Acantharea or Collodaria), or a variety of  
<sup>182</sup> Phaeodarian families (Figure 1). When identification could not be confidently

<sup>183</sup> made between a few candidate taxa, a less specific label was used. As a result,  
<sup>184</sup> we have data from “unidentified Rhizaria”, which typically were vignettes  
<sup>185</sup> not distinguishable between Aulacanthidae or Acantharea or “unidentified  
<sup>186</sup> Phaeodaria”, which are clearly phaeodaria but not distinguishable into a  
<sup>187</sup> family.

<sup>188</sup> The UVP5 samples at ~15Hz rate as it descends the water column and records  
<sup>189</sup> the exact position of each particle larger than  $600\mu m$ . However, identified  
<sup>190</sup> rhizaria ranged from a  $934\mu m$  Aulacanthidae cell to a Collodarian colony over  
<sup>191</sup> 10mm in diameter. To confirm that the UVP5 was sampling adequately across  
<sup>192</sup> all size ranges, an NBSS slope was constructed to identify a drop-off which  
<sup>193</sup> would indicate poor-sampling at the small size range (Barth and Stone, in re-  
<sup>194</sup> view; Lombard et al., 2019). However, it was evident from this analysis that  
<sup>195</sup> all size ranges were adequately sampled across the size range (Supplemental  
<sup>196</sup> Figure 2) so no data were excluded. The UVP5 reports the exact depth at  
<sup>197</sup> which a particle is recorded, however to estimate abundance, observations must  
<sup>198</sup> be binned over fixed depth intervals. Our deployments had variable descent  
<sup>199</sup> depths and speeds with more casts descending to 500m than 1000m and de-  
<sup>200</sup> scents quicker through the epipelagic than the mesopelagic (see Barth and Stone  
<sup>201</sup> (2022) for an extended discussion of UVP5 data processing). For the present  
<sup>202</sup> study, Rhizarian abundances were estimated in 25m vertical bins, which offer  
<sup>203</sup> a moderate sampling volume per bin (average  $0.948m^3$  in the epipelagic and  
<sup>204</sup>  $0.589m^3$  in the mesopelagic) while still maintaining ecologically relevant widths.  
<sup>205</sup> However, concentrations in a 25m bin would need to be greater than 2.428

206 indv.  $m^{-3}$  and 3.912 indv.  $m^{-3}$ , in the epipelagic and mesopelagic respec-  
207 tively, to fall below a 10% non-detection risk [Benfield et al. (1996); Barth and  
208 Stone (in review)]. Because we typically observed many rhizaria taxa below  
209 these concentrations, we present the 25m binned data to visualize broad-scale  
210 average distributions. For quantifying and modelling Rhizaria abundances, we  
211 present integrated abundance estimates, with each cast. Due to the variable  
212 descent depths of the UVP, data are categorized as epipelagic (0-200m), up-  
213 per mesopelagic (200-500m), and lower mesopelagic (500-1000m). The average  
214 sampling volume integrated through these regions were  $7.59m^2$ ,  $7.06m^2$ , and  
215  $11.77m^2$ , with non-detection thresholds at 0.30 indv.  $m^{-2}$ , 0.33 indv.  $m^{-2}$ ,  
216 and 0.20 indv.  $m^{-2}$  respectively. All UVP data processing was done using the  
217 EcotaxaTools package in R (Barth 2023).

## 218 Modelling environmental controls of Rhizarian Abundance

219 Generalized Additive Models (GAMs) were used to assess the relationship  
220 between integrated Rhizarian abundance and different environmental factors.  
221 GAMs offer the ability to model non-linear and non-monotonic relationships,  
222 which can be particularly useful in assessing ecological relationships (Wood,  
223 2017) and have been successfully applied to Rhizarian ecology (Biard and  
224 Ohman, 2020). The mgcv package (Wood, 2001) was used to construct models  
225 relating environmental parameters to each taxonomic group's integrated  
226 abundance estimates from each cast. To select the most parsimonious model  
227 for each analysis, a backwards step-wise approach was taken. First, a full

228 model was fit using any term which may be ecologically relevant. Terms were  
229 fit using maximum likelihood with a double penalty approach on unnecessary  
230 smooths (Marra and Wood, 2011). The smoothness parameter was restricted  
231 ( $k = 6$ ) to prevent overfitting the models. At each iteration of the backwards  
232 step-wise procedure, the model term with the lowest F score (least statistically  
233 significant) was removed. This was repeated until all model terms were  
234 statistically significant or the  $R^2_{adj}$  was substantially reduced. Models were fit  
235 for each region; epipelagic, upper mesopelagic, and lower mesopelagic. In cases  
236 where observations were too sparse for a given taxonomic grouping, models were  
237 not run. All code and full models are available in code, as well as intermediate  
238 data products at <https://github.com/TheAlexBarth/RhizariaSeasonality>.

## 239 Results

### 240 Environmental Variability

241 The BATS sampling region is southeast of Bermuda, situated in the North Sar-  
242 gasso Sea and the North Atlantic oligotrophic ocean gyre. Due to the sampling  
243 location, while the environmental conditions are generally low in variation and  
244 oligotrophic, there is some seasonality and considerable influence from mesoscale  
245 eddies (Lomas et al., 2013; McGillicuddy et al., 1998). Variability in the wa-  
246 ter column structure was visible during the study period (Figure 2). This is  
247 best evidenced through the temperature profiles; In the late summer and early  
248 fall there was a stratified water column with high temperatures in the surface

<sup>249</sup> ( $<75\text{m}$ ) (Figure 2A) and slightly elevated salinity (Figure 2B). This warm, stratified period appeared more intense during the few months sampled in 2019. In <sup>250</sup> 2021, we observed the stratified layer slowly dissipated into the winter months. <sup>251</sup> There was a consistent oxygen minimum zone (OMZ) located at about 750m <sup>252</sup> deep (Figure 2C). Although, February 2021 saw a notable downwelling event, <sup>253</sup> likely due to a passing cyclonic eddy. During this time, warmer, oxic water was <sup>254</sup> plunged deeper into the mesopelagic. This process was reversed in the spring <sup>255</sup> months (March, April) when mixing occurred throughout the epipelagic and the <sup>256</sup> surface was cooler and well mixed. Primary production was highest during the <sup>257</sup> spring mixing period, evidenced both by in-situ fluorescence (Figure 2D) and <sup>258</sup> productivity incubation experiments (Figure 3A). Originating near the surface, <sup>259</sup> the productivity peak moved deeper throughout the spring and declined into <sup>260</sup> the summer (Figure 2D). However, there was a notable, yet smaller productiv- <sup>261</sup> ity bump in the late summer and early fall (Figure 3A) which occurred deeper <sup>262</sup> in the epipelagic (Figure 2D). The particle concentration ( $184\mu\text{m} - 450\mu\text{m}$ ) was <sup>263</sup> closely coupled to chlorophyll-a patterns. <sup>264</sup>

<sup>265</sup> Overall, particle concentration was high near the surface during the 2021 spring <sup>266</sup> bloom, then moved deeper throughout the water column attenuating through- <sup>267</sup> out the lower epipelagic (Figure 2E). Similarly, bacteria abundance was closely <sup>268</sup> linked to overall productivity, although there was a more consistent moderate- <sup>269</sup> abundance layer near the top of the mesopelagic ( $\sim 250\text{m}$ ) (Figure 2F). Con- <sup>270</sup> current with the secondary fall production peak, there was also higher particle <sup>271</sup> concentration and bacterial abundance in the later summer and early fall. In-

terestingly, while primary productivity estimates from July-August were not that different between 2019 and 2021 (Figure 4A), chlorophyll-a florescence, particle concentration, and bacterial abundance were much higher in 2019's summer/fall (Figure 2D-F). Inorganic nutrients (*Si* and *NO<sub>3</sub>*) were generally well stratified, with low concentrations in the epipelagic and increasing throughout the mesopelagic. However, both nutrients did vary vertically in accordance with the 2021 February downwelling and spring mixing period (Figure 2G-H). Additionally, in the late fall of 2021, *Si* concentrations were slightly elevated in the mid-mesopelagic (Figure 2G).

Overall mass flux to the mesopelagic was highest during the 2021 February downwelling (Figure 3B). Generally, export was similarly high during March, declining in April then increasing slightly throughout the summer and early fall. While magnitude was slightly different, this pattern was consistent with total mass, carbon and nitrogen fluxes (Figure 3B-D). Higher mass, carbon and nitrogen flux also occurred in the 2019 late summer - early fall period.

### Rhizaria abundance and distribution

Across all imaged mesozooplankton (>900 $\mu$ m), Rhizaria comprised a considerable fraction of the total community. Considering the total abundances of the observational period, Rhizaria comprised on average, 42.6% of all mesozooplankton abundance (Supplemental Figure 3). Copepods were the second most abundant, comprising 35.5% and all other living mesozooplankton were 22%. The large contribution of Rhizaria to the mesozooplankton community is most

<sup>294</sup> prominent in the epipelagic, where they accounted for 47% of all mesozooplankton.  
<sup>295</sup> In the mesopelagic rhizaria were a smaller fraction, at 38% in the upper  
<sup>296</sup> layers (200-500m) and 37% in the deeper mesopelagic (500-1000m).

<sup>297</sup> Total average Rhizaria abundance had a bimodal distribution with respect to  
<sup>298</sup> depth. Total abundance was highest just below the surface (0-100m), with sec-  
<sup>299</sup> ondary, wider peak occurring in the mid mesopelagic (Figure 4A). Variation in  
<sup>300</sup> depth binned abundance was large, likely due to seasonal variability but also  
<sup>301</sup> increased from the detection-risk described in the methods. The vertical dis-  
<sup>302</sup> tribution pattern and abundance varied considerably across taxonomic groups.

<sup>303</sup> Radiolarians were some of the most abundant taxa observed, particularly in  
<sup>304</sup> the epipelagic (Figure 4, Figure 5B). This pattern was led by Collodaria, whose  
<sup>305</sup> colonies were abundant in the upper epipelagic and declined into the top of  
<sup>306</sup> the mesopelagic (Figure 4C). Acantharea displayed a bimodal distribution ac-  
<sup>307</sup> counting for a large portion of the total Rhizaria pattern (Figure 4B, Figure 5).

<sup>308</sup> Foraminifera had a similar bimodal distribution, yet their overall average den-  
<sup>309</sup> sities were much lower and spread wider throughout the mesopelagic (Figure  
<sup>310</sup> 4E). Phaeodarian families exhibited a wide range of vertical distribution pat-  
<sup>311</sup> terns. The most abundant, Aulacanthidae, also had a bimodal pattern but the  
<sup>312</sup> density was highest in the lower mesopelagic (Figure 4D). Aulosphaeridae had  
<sup>313</sup> low average density and was nearly homogeneously distributed throughout the  
<sup>314</sup> water column, although slightly lower in the epipelagic (Figure 4F). Castanel-  
<sup>315</sup> lidae were the only Phaeodarian who appeared to be effectively restricted to  
<sup>316</sup> the photic zone (Figure 4G). Alternatively, Coelodendridae primarily occurred

<sup>317</sup> in the lower mesopelagic (Figure 4H). A few individuals from the families Tus-  
<sup>318</sup> caroridae and Medusettidae were also observed in the mesopelagic, yet they  
<sup>319</sup> were much rarer (data not shown).

<sup>320</sup> Between the monthly cruises, Rhizaria integrated abundance varied in the  
<sup>321</sup> epipelagic. Highest average abundance occurred in June 2021 and was lowest  
<sup>322</sup> during the winter months (Figure 5A). The 2019 later summer - fall period  
<sup>323</sup> also had much higher integrated abundance than similar months in 2021.

<sup>324</sup> While the majority of integrated abundance in the epipelagic was consistently  
<sup>325</sup> attributable to Collodaria, Acanthrean abundance occurred sporadically and  
<sup>326</sup> could account for a large portion of the total in some months (Figure 5B). The  
<sup>327</sup> mesopelagic integrated abundance was much more consistent across monthly  
<sup>328</sup> cruises, although average abundance was notably higher in 2019 (Figure 5C-F).

<sup>329</sup> The community composition in the mesopelagic was more diverse, mostly  
<sup>330</sup> comprised of Phaeodarians. However, Acantharea and unidentified Rhizaria  
<sup>331</sup> also were common members of the community (Figure 5D, 5F).

<sup>332</sup> **Body size throughout the water column.**

<sup>333</sup> Very few taxa had consistent distributions throughout the water column. Only  
<sup>334</sup> Acanthrea, Foraminifera, Aulacanthidae, and Aulosphaeridae were consistently  
<sup>335</sup> abundant in the epipelagic and mesopelagic. To investigate if the populations  
<sup>336</sup> or morphologies shifted throughout the water column, we compared the sizes  
<sup>337</sup> (Equivalent Spherical Diameters, ESD) between mesopelagic and epipelagic  
<sup>338</sup> groups for each taxa. All groups were significantly different on average (Wilcox

<sup>339</sup> Rank Sum p-value <0.001). Acantharea were smaller, on average in the  
<sup>340</sup> mesopelagic while all other taxa tended to be larger (Figure 6).

<sup>341</sup> **Environmental Drivers of Rhizarian Abundance**

<sup>342</sup> For total Rhizarian integrated abundance the GAMs produced moderate fits  
<sup>343</sup> ( $R^2_{adj} = 0.406\text{--}0.603$ ) (Table 1). In the epipelagic, there were several significant  
<sup>344</sup> predictor variables including inorganic nutrients ( $NO_3$  and  $Si$ ), water quality  
<sup>345</sup> parameters (Salinity, DO), primary production, and particle concentration (Ta-  
<sup>346</sup> ble 1). However, the upper and lower mesopelagic were exclusively explained  
<sup>347</sup> by particle-related variables (concentration and mass flux) (Table 1).

<sup>348</sup> GAMs for individual taxa were much less consistent in their fits (Table 2). This  
<sup>349</sup> is likely in part due to the high number of non-observations for certain taxa.  
<sup>350</sup> Note that due to low abundances, GAMs were not constructed for Tuscaroridae  
<sup>351</sup> or Medusettidae. Furthermore no significant terms were found for a model with  
<sup>352</sup> Aulosphaeridae in the epipelagic nor Foraminifera in the mesopelagic.

<sup>353</sup> Epipelagic Acantharea were explained by several predictor variables and had  
<sup>354</sup> a good fit ( $R^2_{adj} = 0.53$ , Table 2). Most notable smooths were mass flux  
<sup>355</sup> and particle concentration, which had a weak positive association (Figure 7A),  
<sup>356</sup> with July 2021 as a clear outlier where Acantharean abundances were high  
<sup>357</sup> in the epipelagic despite lower fluxes and particle concentrations (Figure 5).

<sup>358</sup> Foraminifera had a good fitting GAM in the epipelagic ( $R^2_{adj} = 0.445$ ). There  
<sup>359</sup> were several significant explanatory variables, although the clearest pattern was  
<sup>360</sup> observed of high temperatures associated with more Foraminifera abundance

<sup>361</sup> (Table 2, Figure 7B). Epipelagic Aulacanthidae similarly had several predictor  
<sup>362</sup> variables which were significant, including both water quality parameters and  
<sup>363</sup> particle/flux predictors (Table 2). Interestingly, Aulacanthidae had primary  
<sup>364</sup> production as a significant predictor, yet there was not a clear association (Figure  
<sup>365</sup> 7C). There was a fit for Collodaria in the epipelagic ( $R^2_{adj} = 0.16$ ), although  
<sup>366</sup> there was a logit-like relationship where higher abundances tended to occur dur-  
<sup>367</sup> ing higher DO conditions in the surface waters (Figure 7D). Castanellidae also  
<sup>368</sup> had similarly poor fits in the epipelagic ( $R^2_{adj} = 0.124$ ) (Table 2, Figure 7E).

<sup>369</sup> In the upper mesopelagic (200-500m), abundances were generally low (Figure  
<sup>370</sup> 4) so GAMs were only constructed for Acantharea, Aulacanthidae, Aulosphaeri-  
<sup>371</sup> dae, and Coelodendridae (Table 2). All these models had generally poor fits  
<sup>372</sup> ( $R^2_{adj} < 0.25$ ). Yet, for all upper mesopelagic models, particle concentration  
<sup>373</sup> was a significant explanatory variable (Table 2, Figure 8). Carbon flux was sig-  
<sup>374</sup> nificant for Acantharea and nitrogen flux was significant for both Acantharea  
<sup>375</sup> and Coelodendridae (Table 2, Figure 8A,D). The lower mesopelagic also had  
<sup>376</sup> generally poor GAM fits for taxa specific models ( $R^2_{adj} < 0.3$ ), with the excep-  
<sup>377</sup> tion of Acantharea ( $R^2_{adj} = 0.509$ ). Acantharea in the lower mesopelagic was  
<sup>378</sup> most clearly positively associated with particle concentration and nitrogen flux,  
<sup>379</sup> as well as temperature to a slight degree (Figure 9A). For all Phaeodarians with  
<sup>380</sup> a significant model, particle concentration was a main predictor variable (Table  
<sup>381</sup> 2, Figure 9B-D). Aulacanthidae had the best fitting model of the Phaeodari-  
<sup>382</sup> ans ( $R^2_{adj} = 0.298$ ), which also included mass flux as a statistically significant  
<sup>383</sup> smooth (Figure 9B).

<sup>384</sup> **Discussion**

<sup>385</sup> **Overall Rhizarian abundance and patterns**

<sup>386</sup> In the epipelagic Rhizaria exhibited a notable seasonal pattern. Rhizarian abun-  
<sup>387</sup> dances were higher in the summer months and lower during the winter. During  
<sup>388</sup> a prior time period, Blanco-Bercial et al. (2022) noted that there is considerable  
<sup>389</sup> seasonality in the community composition of all protists. Despite the seasonality  
<sup>390</sup> of total Rhizarian abundance, community composition was relatively consistent,  
<sup>391</sup> with Collodaria representing the bulk of the community. It should be noted that  
<sup>392</sup> the overall taxonomic resolution of the UVP5 is fairly low, so there may be a  
<sup>393</sup> switching of species within the broad groups identified in this study which were  
<sup>394</sup> not captured. Throughout the mesopelagic, month-to-month variation in 2021  
<sup>395</sup> was relatively low. Again this is consistent with observations from metabarcod-  
<sup>396</sup> ing of the whole protist community in the same study region (Blanco-Bercial  
<sup>397</sup> et al., 2022). This finding is not surprising as the overall seasonal variation in  
<sup>398</sup> environmental conditions in this region were low.

<sup>399</sup> Overall Rhizaria were the most commonly identified group of mesozooplankton  
<sup>400</sup> throughout the study period. We do note that the UVP5 commonly captures  
<sup>401</sup> Trichodesmium colonies, yet these were excluded in this comparison as they are  
<sup>402</sup> strictly autotrophs. It should be noted that previous work has suggested that  
<sup>403</sup> avoidance behavior with the UVP is possible, at times likely, for visual and  
<sup>404</sup> highly mobile zooplankton (Barth and Stone, 2022). Thus, the percent contri-  
<sup>405</sup> bution reported here (42.7%) of Rhizaria to the total mesozooplankton commu-

406 nity may be inflated due to under sampling of organisms such as Euphausiids  
407 and Chaetognaths which have quick escape responses. Regardless, it is worth  
408 noting that in the same region, with data collected in 2012 and 2013 using  
409 similar calculation methods, Biard et al. (2016) estimated Rhizaria only con-  
410 tribute 15% of the total mesozooplankton community in the upper 500m. Likely,  
411 Rhizaria display considerable interannual variability. In the present study, we  
412 noticed considerably higher Rhizarian abundance throughout the water column  
413 in 2019 compared to 2021. While this may have been driven by increased mass  
414 flux, more information is needed to truly understand the magnitude by which  
415 Rhizaria can vary interannually.

416 **Relationship to environmental parameters**

417 In general, the fit of most GAMs were moderate to poor. One possible reason  
418 for the poor fits may have been that for some taxa, conditions were not variable  
419 enough to capture a range of conditions at which they may exist. For instance,  
420 Collodaria were the most abundant taxa observed, yet the fit of their GAM  
421 was particularly poor. In studies which covered a wider range of parameters,  
422 Collodaria has been shown to strongly vary with changes in parameters such as  
423 temperature, chlorophyll-a, mixing, and water clarity (Biard et al., 2017; Biard  
424 and Ohman, 2020). Alternatively, Acantharea had relatively good fitting GAMs.  
425 These taxa also had some of the largest variation from month to month on  
426 cruises. Thus, it may be that in the oligotrophic, the relatively stable conditions  
427 can support certain taxa while others are more sporadic. It should also be noted

428 that due to the challenge of adequately sampling enough volume to overcome  
429 low-detection issues, GAMs were run on integrated data. However, variation  
430 with environmental parameters throughout the water column are likely, just  
431 not captured in the modelling aspect of this study. One consistent parameter  
432 which had significant positive associations was particle concentration. This  
433 observation is not surprising as most rhizaria likely to some extent engage in  
434 flux feeding.

435 **Vertical Structure and Trophic Roles**

436 In this study we present a clear pattern of vertical zonation between different  
437 Rhizaria groups. Largely, the taxonomic composition and vertical positioning  
438 were similar to Rhizaria zonation in the California Current Ecosystem (Biard  
439 and Ohman, 2020). It should be noted however, that the secondary abun-  
440 dance peak reported in the present study is lower. This is likely due to the  
441 more oligotrophic nature of the study region, where the euphotic zone penetrates  
442 deeper into the water column. Most prevalent in the epipelagic were Collo-  
443 daria. These mixotrophic Radiolarians have long been reported to contribute  
444 to primary productivity in the euphotic zone (Dennett et al., 2002; Michaels et  
445 al., 1995). Collodaria are thought to be particularly successful globally in olig-  
446 otrophic regions due to their photosymbiotic relationships (Biard et al., 2017,  
447 2016). We observed the highest abundance of Collodaria during June 2021,  
448 supporting the notion they can thrive during the typically low-nutrient condi-  
449 tions of summer stratification. However, Collodaria also increased during the

450 spring mixing period, suggesting that they can thrive during conditions which  
451 may typically be thought to favor autotrophs. Furthermore, while Collodaria  
452 were primarily absent from below 250m, there were a few instances of deeper  
453 colonies being observed. Global investigations of polycystine flux, suggest that  
454 deep-Collodaria in Oligotrophic regions may be a consequence of isothermal sub-  
455 mersion (Boltovskoy, 2017). Another effectively exclusively epipelagic Rhizaria  
456 was the Phaeodarian family of Castanellidae. All Phaeodarians are thought to  
457 be fully heterotrophic (Nakamura and Suzuki, 2015), nonetheless a number of  
458 studies, including this one, report Castanellidae to be typically found in the  
459 lower epipelagic (Biard et al., 2018; Biard and Ohman, 2020; Zasko and Ru-  
460 sanov, 2005). It should be considered that perhaps Castanellidae specializes in  
461 feeding on sinking particles directly at the base of the epipelagic. Given it's  
462 smaller size (Nakamura and Suzuki, 2015), Castanellidae does not need a large  
463 diameter to efficiently flux feed at the typically particle rich region of the lower  
464 epipelagic. Both Castanellidae and Collodaria had poor fitting GAMs. This is  
465 somewhat of a surprise for Collodaria who had large abundance. However, given  
466 the consistency of their abundance, it may be that this study did not capture a  
467 wide enough range of conditions for describing Collodaria's preferred niche.

468 The mesopelagic generally was home to known heterotrophic organisms,  
469 particularly for those which were constrained to exclusively occupy deeper  
470 waters. This is consistent with Blanco-Bercial et al. (2022)'s observation of  
471 an auto-/mixotroph to heterotroph gradient in the protist community. The  
472 upper mesopelagic interestingly had relatively low total abundance. This

473 low-abundance region likely reflects the dynamics of productivity and export  
474 throughout the water column. While productivity and thus sinking particles for  
475 flux feeders are high in the euphotic zone, much of this is attenuated throughout  
476 the epipelagic. So, while the base of the epipelagic may provide a rich feeding  
477 environment for Castanellidae, smaller protists, or heterotrophic bacteria  
478 (Figure 2F), the region from 200-500m might be otherwise food poor. Perhaps  
479 it is more advantageous for Rhizaria to situate deeper, in darker regions of the  
480 twilight zone. Also it should be noted that Phaeodarians utilize silica to build  
481 their opaline tests, and silica concentrations started to increase around 500m  
482 (Figure 2G). Although *Si* was not a significant smooth for any taxa-specific  
483 model, this lack of association might be due to the overall lack of variation of *Si*  
484 between integrated abundance of each cast. Aulosphaeridae was only found to  
485 have significant relationships, although weak fits, to particle concentration in  
486 the mesopelagic. In our study, while consistently observed, overall abundances  
487 of Aulosphaeridae were very low. In the Pacific Ocean, on California's Coast,  
488 much higher abundances of Aulosphaeridae have been reported (Biard and  
489 Ohman, 2020; Zasko and Rusanov, 2005) and they have massive potential to  
490 impact silica export (Biard et al., 2018). Coelodendridae were also seemingly  
491 restricted to the deeper section of the mesopelagic. This is interesting given  
492 that in the California Current, (Biard and Ohman, 2020) found a bimodal  
493 distribution in Coelodendridae. There are several morphotypes corresponding  
494 to different taxa of Coelodendridae (Biard and Ohman, 2020; Nakamura and  
495 Suzuki, 2015). So it may be that only a few types of Coelodendridae were

<sup>496</sup> observed in this study, while the epipelagic variety was not. Alternatively, the  
<sup>497</sup> lower epipelagic of the California Current may provide adequate habitat for  
<sup>498</sup> Coelodendridae, which is not available in the oligotrophic Sargasso Sea.

<sup>499</sup> A number of taxa were found to have a bimodal distribution, with considerable  
<sup>500</sup> populations in both the epipelagic and mesopelagic. Aulacanthidae had a bi-  
<sup>501</sup> modal distribution, although abundances were highest in the lower mesopelagic.  
<sup>502</sup> Foraminifera also had a bimodal distribution. Some lineages of Foraminifera  
<sup>503</sup> are known to host photosymbionts (Biard, 2022a; Kimoto, 2015), however they  
<sup>504</sup> are also efficient predators commonly seen throughout the mesopelagic (Caron  
<sup>505</sup> and Be, 1984; Gaskell et al., 2019). Thus it is not surprising to find their pres-  
<sup>506</sup> ence in both locations of the water column. Foraminifera are also known to  
<sup>507</sup> vary their vertical distribution across their life cycle in phase with lunar cycles  
<sup>508</sup> (Biard, 2022a; Bijma et al., 1990; Gaskell et al., 2019; Kimoto, 2015). However,  
<sup>509</sup> the sampling scheme of the BATS program does not capture this frequency and  
<sup>510</sup> was not investigated in the present study.

<sup>511</sup> Acantharea also had a bimodal distribution, with much larger abundances than  
<sup>512</sup> Aulacanthidae or Foraminifera. Most prior studies of Acantharea vertical dis-  
<sup>513</sup> tribution found them concentrated in near surface layers of the water column  
<sup>514</sup> Zasko and Rusanov (2005). This would support the paradigm that large Acan-  
<sup>515</sup> tharean abundances may be supported by their mixotrophic abilities (Michaels  
<sup>516</sup> et al., 1995; Suzuki and Not, 2015). While the UVP5 images cannot distinguish  
<sup>517</sup> between mixotrophic and heterotrophic Acantharea, the GAMs constructed for  
<sup>518</sup> Acantharean abundance found positive associations with particle concentration

519 and mass flux, suggesting a higher reliance on heterotrophy. Recently Mars Bris-  
520 bin et al. (2020) described apparent predator behavior amongst near-surface  
521 Acantharea. Thus it is likely that epipelagic Acantharea may commonly be  
522 heterotrophic. Yet, it should be noted in the Sargasso Sea, both heterotrophic  
523 and symbiotic lineages of Acantharea have been reported (Blanco-Bercial et al.,  
524 2022). Additionally, Michaels (1988) noted that the majority of Acantharea (by  
525 abundance) were smaller than  $160\mu m$ . While that estimate may be inflated due  
526 to inability to capture larger cells, small Acantharea were not captured in the  
527 present study. Thus, trophic strategy may shift based on sizes of Acantharea.  
  
528 Decelle et al. (2013) proposed a hypothetical life cycle for cyst-bearing  
529 (strictly heterotrophic) Acantharea. This hypothesized life cycle suggests that  
530 epipelagic Acantharea are adult populations, which form cysts that sink into  
531 the mesopelagic, then reproduce and rise. Furthermore, given that horizontal  
532 transfer of symbionts between generations of Acantharea is unlikely due to  
533 their spawning behavior, the newly spawned mesopelagic Acantharea are not  
534 necessarily required to rapidly return to the photic zone (Decelle et al., 2013,  
535 2012). This hypothesis predicts that Acanthareans in the mesopelagic would be  
536 smaller (Decelle et al., 2013). Mars Brisbin et al. (2020) provided some support  
537 for this hypothesis, with a significant decrease in Acantharea sizes with depth.  
  
538 Although the authors also observed low abundances in the mesopelagic and  
539 noted that the smaller sizes may be due to lower food availability (Mars Brisbin  
540 et al., 2020). Since food is more scarce in the mesopelagi, nutritional quality  
541 lower, yet flux feeders would likely grow larger to increase their feeding range

542 (Biard and Ohman, 2020). In the data collecting in this study, Acanthareans  
543 in the mesopelagic were significantly smaller than the epipelagic, despite the  
544 other bimodal taxa (Foraminifera and Aulacanthidae) being significantly larger  
545 with depth. This provides added support for the hypothesis that cyst-forming  
546 Acantharea may utilize different sections of the water column throughout their  
547 life cycle. However to further investigate this, more work is needed with higher  
548 temporal and taxonomic resolution.

549 **Conclusions and Considerations**

550 This study provides a detailed look at Rhizarian abundance over time through-  
551 out the water column in a major oligotrophic gyre. We show that their abun-  
552 dances are generally related to particle concentration and flux, although lack  
553 of environmental variability may have reduced the fit of our GAMs. Consid-  
554 ering the potential role of Rhizaria in the biological carbon pump, they may  
555 have a somewhat mixed role. In the shallower regions, where smaller Rhizaria  
556 are abundant, they may be an attenuating force on sinking particles (Stukel  
557 et al., 2019). It should be noted that in our study, we focused on the “small”  
558 particle concentration field ( $<450\mu m$ ), and these particles are generally slower  
559 sinking than large particles. However, once consumed and repackaged by larger  
560 Rhizaria, they can sink quicker and contribute more to overall flux (Michaels,  
561 1988). Thus, Rhizaria may act as an aggregation mechanism. However, this is  
562 largely speculation, to truly test this, more work is needed measuring Rhizarian  
563 flux.

564 The vertical partitioning documented in this study do support the hypothesis  
565 that mixotrophic rhizaria will occupy shallower waters while deeper waters are  
566 dominated by heterotrophy. However the degree to which mixotrophic Rhizaria  
567 in the euphotic zone rely on heterotrophy versus symbiosis is uncertain. Col-  
568 lodaria were recorded as consistent and dominant members of the near surface  
569 region. These organisms have the potential to contribute considerably to the oth-  
570 erwise low productivity of oligotrophic regions. However, their role in food webs  
571 is not well understood. While this study represents a step-forward in our under-  
572 standing of Rhizarian ecology, continued research on Rhizaria is much needed  
573 to better understand their ecology. Particularly extended descriptive work to  
574 capture interannual patterns. Also work defining biotic interactions, feeding  
575 rates, productivity, and life history are all rich fields of interest in Rhizaria.

## 576 References:

- 577 Anderson, O.R., 2014. Living Together in the Plankton: A Survey of Marine  
578 Protist Symbioses. *Acta Protozoologica* 53, 29–38. <https://doi.org/10.4467/16890027AP.13.0019.1116>
- 580 Anderson, O.R., Bé, A.W.H., 1976. A CYTOCHEMICAL FINE STRUCTURE  
581 STUDY OF PHAGOTROPHY IN A PLANKTONIC FORAMINIFER,  
582 *HASTIGERINA PELAGICA* (d'ORBIGNY). *The Biological Bulletin* 151,  
583 437–449. <https://doi.org/10.2307/1540498>
- 584 Aurahs, R., Grimm, G.W., Hemleben, V., Hemleben, C., Kucera, M., 2009. Ge-  
585 graphical distribution of cryptic genetic types in the planktonic foraminifer

- 586 Globigerinoides ruber. Molecular Ecology 18, 1692–1706. <https://doi.org/10.1111/j.1365-294X.2009.04136.x>
- 587 Barth, A., Stone, J., in review. Understanding the picture: The promises and challenges of in-situ imagery data in the study of plankton ecology.
- 588 Barth, A., Stone, J., 2022. Comparison of an in situ imaging device and net-based method to study mesozooplankton communities in an oligotrophic system. Frontiers in Marine Science 9.
- 589 Benfield, M.C., Davis, C.S., Wiebe, P.H., Gallager, S.M., Gregory Lough, R., Copley, N.J., 1996. Video Plankton Recorder estimates of copepod, pteropod and larvacean distributions from a stratified region of Georges Bank with comparative measurements from a MOCNESS sampler. Deep Sea Research Part II: Topical Studies in Oceanography 43, 1925–1945. [https://doi.org/10.1016/S0967-0645\(96\)00044-6](https://doi.org/10.1016/S0967-0645(96)00044-6)
- 590 Biard, T., 2022a. Rhizaria. Encyclopedia of Life Sciences, pp. 1–11. <https://doi.org/10.1002/9780470015902.a0029469>
- 591 Biard, T., 2022b. Diversity and ecology of Radiolaria in modern oceans. Environmental Microbiology 24, 2179–2200. <https://doi.org/10.1111/1462-2920.16004>
- 592 Biard, T., Bigeard, E., Audic, S., Poulain, J., Gutierrez-Rodriguez, A., Pesant, S., Stemmann, L., Not, F., 2017. Biogeography and diversity of Collodaria (Radiolaria) in the global ocean. The ISME Journal 11, 1331–1344. <https://doi.org/10.1038/ismej.2017.12>
- 593 Biard, T., Krause, J.W., Stukel, M.R., Ohman, M.D., 2018. The Significance

of Giant Phaeodarians (Rhizaria) to Biogenic Silica Export in the California Current Ecosystem. *Global Biogeochemical Cycles* 32, 987–1004. <https://doi.org/10.1029/2018GB005877>

Biard, T., Ohman, M.D., 2020. Vertical niche definition of test-bearing protists (Rhizaria) into the twilight zone revealed by in situ imaging. *Limnology and Oceanography* 65, 2583–2602. <https://doi.org/10.1002/lno.11472>

Biard, T., Pillet, L., Decelle, J., Poirier, C., Suzuki, N., Not, F., 2015. Towards an integrative morpho-molecular classification of the colloidaria (polycystinea, radiolaria). *Protist* 166, 374–388. <https://doi.org/10.1016/j.protis.2015.05.002>

Biard, T., Stemmann, L., Picheral, M., Mayot, N., Vandromme, P., Hauss, H., Gorsky, G., Guidi, L., Kiko, R., Not, F., 2016. In situ imaging reveals the biomass of giant protists in the global ocean. *Nature* 532, 504–507. <https://doi.org/10.1038/nature17652>

Bijma, J., Erez, J., Hemleben, C., 1990. **Lunar and semi-lunar reproductive cycles in some spinose planktonic foraminifers.** *Journal of Foraminiferal Research* 20, 117–127.

Blanco-Bercial, L., Parsons, R., Bolaños, L.M., Johnson, R., Giovannoni, S.J., Curry, R., 2022. **The protist community traces seasonality and mesoscale hydrographic features in the oligotrophic sargasso sea.** *Frontiers in Marine Science* 9.

Boltovskoy, D., 2017. Vertical distribution patterns of radiolaria polycystina (protista) in the world ocean: Living ranges, isothermal submersion and

- 632 settling shells. Journal of Plankton Research 39, 330–349. <https://doi.org/10.1093/plankt/fbx003>
- 633
- 634 Boltovskoy, D., Alder, V.A., Abelmann, A., 1993. Annual flux of radiolaria and  
635 other shelled plankters in the eastern equatorial atlantic at 853 m: seasonal  
636 variations and polycystine species-specific responses. Deep Sea Research  
637 Part I: Oceanographic Research Papers 40, 1863–1895. [https://doi.org/10.1016/0967-0637\(93\)90036-3](https://doi.org/10.1016/0967-0637(93)90036-3)
- 638
- 639 Caron, D.A., 2016. The rise of rhizaria | nature. Nature 532, 444–445.
- 640 Caron, D.A., Be, A.W.H., 1984. PREDICTED AND OBSERVED FEEDING  
641 RATES OF THE SPINOSE PLANKTONIC FORAMINIFER. BULLETIN  
642 OF MARINE SCIENCE 35.
- 643 Caron, D.A., Michaels, A.F., Swanberg, N.R., Howse, F.A., 1995. Primary pro-  
644 ductivity by symbiont-bearing planktonic sarcodines (acantharia, radiolaria,  
645 foraminifera) in surface waters near bermuda. Journal of Plankton Research  
646 17, 103–129. <https://doi.org/10.1093/plankt/17.1.103>
- 647 Cavalier-Smith, T., Chao, E.E., Lewis, R., 2018. Multigene phylogeny and cell  
648 evolution of chromist infrakingdom Rhizaria: contrasting cell organisation of  
649 sister phyla Cercozoa and Retaria. Protoplasma 255, 1517–1574. <https://doi.org/10.1007/s00709-018-1241-1>
- 650
- 651 Cohen, N.R., Krinos, A.I., Kell, R.M., Chmiel, R.J., Moran, D.M., McIlvin,  
652 M.R., Lopez, P.Z., Barth, A., Stone, J., Alanis, B.A., Chan, E.W., Breier,  
653 J.A., Jakuba, M.V., Johnson, R., Alexander, H., Saito, M.A., 2023. Mi-  
654 croeukaryote metabolism across the western North Atlantic Ocean revealed

655 through autonomous underwater profiling. <https://doi.org/10.1101/2023.11.20.567900>

656 Decelle, J., Colin, S., Foster, R.A., 2015. Photosymbiosis in Marine Planktonic  
657 Protists, in: Ohtsuka, S., Suzuki, T., Horiguchi, T., Suzuki, N., Not, F.  
658 (Eds.), Springer Japan, Tokyo, pp. 465–500. [https://doi.org/10.1007/978-4-431-55130-0\\_19](https://doi.org/10.1007/978-4-431-55130-0_19)

660 Decelle, J., Martin, P., Paborstava, K., Pond, D.W., Tarling, G., Mahé, F., De  
661 Vargas, C., Lampitt, R., Not, F., 2013. Diversity, Ecology and Biogeochemistry  
662 of Cyst-Forming Acantharia (Radiolaria) in the Oceans. PLoS ONE 8,  
663 e53598. <https://doi.org/10.1371/journal.pone.0053598>

664 Decelle, J., Siano, R., Probert, I., Poirier, C., Not, F., 2012. Multiple microalgal  
665 partners in symbiosis with the acantharian *Acanthochiasma* sp. (Radiolaria).  
666 Symbiosis 58, 233–244. <https://doi.org/10.1007/s13199-012-0195-x>

667 Dennett, M.R., Caron, D.A., Michaels, A.F., Gallager, S.M., Davis, C.S., 2002.  
668 Video plankton recorder reveals high abundances of colonial radiolaria in  
669 surface waters of the central north pacific. Journal of Plankton Research 24,  
670 797–805. <https://doi.org/10.1093/plankt/24.8.797>

671 Drago, L., Panaïotis, T., Irisson, J.-O., Babin, M., Biard, T., Carlotti, F.,  
672 Coppola, L., Guidi, L., Hauss, H., Karp-Boss, L., Lombard, F., McDonnell,  
673 A.M.P., Picheral, M., Rogge, A., Waite, A.M., Stemmann, L., Kiko,  
674 R., 2022. Global Distribution of Zooplankton Biomass Estimated by In  
675 Situ Imaging and Machine Learning. Frontiers in Marine Science 9. <https://doi.org/10.3389/fmars.2022.894372>

- 678 Gaskell, D.E., Ohman, M.D., Hull, P.M., 2019. Zooglider-based measurements  
679 of planktonic foraminifera in the California Current System. *Journal of*  
680 *Foraminiferal Research* 49, 390–404. <https://doi.org/10.2113/gsjfr.49.4.390>
- 681 Guidi, L., Chaffron, S., Bittner, L., Eveillard, D., Larhlimi, A., Roux, S.,  
682 Darzi, Y., Audic, S., Berline, L., Brum, J.R., Coelho, L.P., Espinoza, J.C.I.,  
683 Malviya, S., Sunagawa, S., Dimier, C., Kandels-Lewis, S., Picheral, M.,  
684 Poulain, J., Searson, S., Stemmann, L., Not, F., Hingamp, P., Speich, S.,  
685 Follows, M., Karp-Boss, L., Boss, E., Ogata, H., Pesant, S., Weissenbach, J.,  
686 Wincker, P., Acinas, S.G., Bork, P., Vargas, C. de, Iudicone, D., Sullivan,  
687 M.B., Raes, J., Karsenti, E., Bowler, C., Gorsky, G., 2016. Plankton net-  
688 works driving carbon export in the oligotrophic ocean. *Nature* 532, 465–470.  
689 <https://doi.org/10.1038/nature16942>
- 690 Gutierrez-Rodriguez, A., Stukel, M.R., Lopes dos Santos, A., Biard, T., Scharek,  
691 R., Vaulot, D., Landry, M.R., Not, F., 2019. High contribution of Rhizaria  
692 (Radiolaria) to vertical export in the California Current Ecosystem revealed  
693 by DNA metabarcoding. *The ISME Journal* 13, 964–976. <https://doi.org/10.1038/s41396-018-0322-7>
- 694 Gutiérrez-Rodríguez, A., Lopes dos Santos, A., Safi, K., Probert, I., Not, F.,  
695 Fernández, D., Gourvil, P., Bilewitch, J., Hulston, D., Pinkerton, M., Nod-  
696 der, S.D., 2022. Planktonic protist diversity across contrasting subtropical  
697 and subantarctic waters of the southwest Pacific. *Progress in Oceanography*  
698 206, 102809. <https://doi.org/10.1016/j.pocean.2022.102809>
- 699 700 Haekel, E., 1887. *Report on the radiolaria collected by H.M.S. Challenger during*

701 the years 1873-1876, plates, by ernst haeckel.

702 Hull, P.M., Osborn, K.J., Norris, R.D., Robison, B.H., 2011. Seasonality and  
703 depth distribution of a mesopelagic foraminifer, *Hastigerinella digitata*, in  
704 Monterey Bay, California. Limnology and Oceanography 56, 562–576. <https://doi.org/10.4319/lo.2011.56.2.0562>

705 Ikenoue, T., Kimoto, K., Okazaki, Y., Sato, M., Honda, M.C., Takahashi, K.,  
706 Harada, N., Fujiki, T., 2019. Phaeodaria: An Important Carrier of Particu-  
707 late Organic Carbon in the Mesopelagic Twilight Zone of the North Pacific  
708 Ocean. Global Biogeochemical Cycles 33, 1146–1160. <https://doi.org/10.1029/2019GB006258>

709 Kimoto, K., 2015. Planktic foraminifera. pp. 129–178. [https://doi.org/10.1007/978-4-431-55130-0\\_7](https://doi.org/10.1007/978-4-431-55130-0_7)

710 Lampitt, R.S., Salter, I., Johns, D., 2009. Radiolaria: Major exporters of or-  
711 ganic carbon to the deep ocean. Global Biogeochemical Cycles 23. <https://doi.org/10.1029/2008GB003221>

712 Lee, J.J., 2006. *Algal symbiosis in larger foraminifera*. Symbiosis 42, 63–75.

713 Llopis Monferrer, N., Biard, T., Sandin, M.M., Lombard, F., Picheral, M., Elin-  
714 eau, A., Guidi, L., Leynaert, A., Tréguer, P.J., Not, F., 2022. *Siliceous*  
715 *rhizaria abundances and diversity in the mediterranean sea assessed by com-*  
716 *bined imaging and metabarcoding approaches*. Frontiers in Marine Science  
717 9.

718 Llopis Monferrer, N., Leynaert, A., Tréguer, P., Gutiérrez-Rodríguez, A.,  
719 Moriceau, B., Gallinari, M., Latasa, M., L'Helguen, S., Maguer, J.-F., Safi,

- 724 K., Pinkerton, M.H., Not, F., 2021. Role of small Rhizaria and diatoms  
725 in the pelagic silica production of the Southern Ocean. Limnology and  
726 Oceanography 66, 2187–2202. <https://doi.org/10.1002/lno.11743>
- 727 Lomas, M.W., Bates, N.R., Johnson, R.J., Knap, A.H., Steinberg, D.K., Carl-  
728 son, C.A., 2013. Two decades and counting: 24-years of sustained open ocean  
729 biogeochemical measurements in the Sargasso Sea. Deep Sea Research Part  
730 II: Topical Studies in Oceanography 93, 16–32. <https://doi.org/10.1016/j.dsr2.2013.01.008>
- 731
- 732 Lombard, F., Boss, E., Waite, A.M., Vogt, M., Uitz, J., Stemmann, L., Sosik,  
733 H.M., Schulz, J., Romagnan, J.-B., Picheral, M., Pearlman, J., Ohman,  
734 M.D., Niehoff, B., Möller, K.O., Miloslavich, P., Lara-Lpez, A., Kudela, R.,  
735 Lopes, R.M., Kiko, R., Karp-Boss, L., Jaffe, J.S., Iversen, M.H., Irisson,  
736 J.-O., Fennel, K., Hauss, H., Guidi, L., Gorsky, G., Giering, S.L.C., Gaube,  
737 P., Gallager, S., Dubelaar, G., Cowen, R.K., Carlotti, F., Briseño-Avena,  
738 C., Berline, L., Benoit-Bird, K., Bax, N., Batten, S., Ayata, S.D., Artigas,  
739 L.F., Appeltans, W., 2019. [Globally consistent quantitative observations of](#)  
740 [planktonic ecosystems](#). Frontiers in Marine Science 6.
- 741 Marra, G., Wood, S.N., 2011. Practical variable selection for generalized ad-  
742 ditive models. Computational Statistics & Data Analysis 55, 2372–2387.  
743 <https://doi.org/10.1016/j.csda.2011.02.004>
- 744 Mars Brisbin, M., Brunner, O.D., Grossmann, M.M., Mitarai, S., 2020. Paired  
745 high-throughput, in situ imaging and high-throughput sequencing illuminate  
746 acantharian abundance and vertical distribution. Limnology and Oceanog-

- 747       raphy 65, 2953–2965. <https://doi.org/10.1002/lno.11567>
- 748       McGillicuddy, D.J., Robinson, A.R., Siegel, D.A., Jannasch, H.W., Johnson,
- 749       R., Dickey, T.D., McNeil, J., Michaels, A.F., Knap, A.H., 1998. Influence
- 750       of mesoscale eddies on new production in the Sargasso Sea. Nature 394,
- 751       263–266. <https://doi.org/10.1038/28367>
- 752       Michaels, A.F., 1988. Vertical distribution and abundance of Acantharia and
- 753       their symbionts. Marine Biology 97, 559–569. <https://doi.org/10.1007/BF00391052>
- 754       Michaels, A.F., Caron, D.A., Swanberg, N.R., Howse, F.A., Michaels, C.M.,
- 755       1995. Planktonic sarcodines (Acantharia, Radiolaria, Foraminifera) in sur-
- 756       face waters near Bermuda: abundance, biomass and vertical flux. Journal of
- 757       Plankton Research 17, 131–163. <https://doi.org/10.1093/plankt/17.1.131>
- 758       Michaels, A.F., Knap, A.H., 1996. Overview of the U.S. JGOFS Bermuda
- 759       Atlantic Time-series Study and the Hydrostation S program. Deep Sea
- 760       Research Part II: Topical Studies in Oceanography 43, 157–198. [https://doi.org/10.1016/0967-0645\(96\)00004-5](https://doi.org/10.1016/0967-0645(96)00004-5)
- 761       Nakamura, Y., Itagaki, H., Tuji, A., Shimode, S., Yamaguchi, A., Hidaka,
- 762       K., Ogiso-Tanaka, E., 2023. DNA metabarcoding focused on difficult-to-
- 763       culture protists: An effective approach to clarify biological interactions.
- 764       Environmental Microbiology 25, 3630–3638. <https://doi.org/10.1111/1462-2920.16524>
- 765       Nakamura, Y., Suzuki, N., 2015. **Phaeodaria: Diverse marine cercozoans of**
- 766       **world-wide distribution.** Springer, pp. 223–249.
- 767

- 770 Ohman, M.D., 2019. A sea of tentacles: optically discernible traits resolved from  
771 planktonic organisms in situ. ICES Journal of Marine Science 76, 1959–1972.  
772 <https://doi.org/10.1093/icesjms/fsz184>
- 773 Panaïotis, T., Babin, M., Biard, T., Carlotti, F., Coppola, L., Guidi, L., Hauss,  
774 H., Karp-Boss, L., Kiko, R., Lombard, F., McDonnell, A.M.P., Picheral, M.,  
775 Rogge, A., Waite, A.M., Stemmann, L., Irisson, J.-O., 2023. Three major  
776 mesoplanktonic communities resolved by in situ imaging in the upper 500  
777 m of the global ocean. Global Ecology and Biogeography 32, 1991–2005.  
778 <https://doi.org/10.1111/geb.13741>
- 779 Picheral, M., Colin, S.P., Irisson, J.-O., n.d. [Ecotaxa](#).
- 780 Picheral, M., Guidi, L., Stemmann, L., Karl, D.M., Iddaoud, G., Gorsky, G.,  
781 2010. The Underwater Vision Profiler 5: An advanced instrument for high  
782 spatial resolution studies of particle size spectra and zooplankton. Limnology  
783 and Oceanography: Methods 8, 462–473. <https://doi.org/10.4319/lom.2010.8.462>
- 784 [8.462](#)
- 785 Sogawa, S., Nakamura, Y., Nagai, S., Nishi, N., Hidaka, K., Shimizu, Y., Setou,  
786 T., 2022. DNA metabarcoding reveals vertical variation and hidden diversity  
787 of alveolata and rhizaria communities in the western north pacific. Deep  
788 Sea Research Part I: Oceanographic Research Papers 183, 103765. <https://doi.org/10.1016/j.dsr.2022.103765>
- 790 Stukel, M.R., Biard, T., Krause, J., Ohman, M.D., 2018. Large Phaeodaria in  
791 the twilight zone: Their role in the carbon cycle. Limnology and Oceanog-  
792 raphy 63, 2579–2594. <https://doi.org/10.1002/lno.10961>

- 793 Stukel, M.R., Ohman, M.D., Kelly, T.B., Biard, T., 2019. The roles of  
794 suspension-feeding and flux-feeding zooplankton as gatekeepers of particle  
795 flux into the mesopelagic ocean in the northeast pacific. Frontiers in Marine  
796 Science 6.
- 797 Suzuki, N., Not, F., 2015. Biology and ecology of radiolaria. Springer, pp.  
798 179–222.
- 799 Swanberg, N.R., Anderson, O.R., 1981. Collozoum caudatum sp. nov.: A  
800 giant colonial radiolarian from equatorial and Gulf Stream waters. Deep  
801 Sea Research Part A. Oceanographic Research Papers 28, 1033–1047. [https://doi.org/10.1016/0198-0149\(81\)90016-9](https://doi.org/10.1016/0198-0149(81)90016-9)
- 802 803 Takahashi, K., Hurd, D.C., Honjo, S., 1983. Phaeodarian skeletons: Their role  
804 in silica transport to the deep sea. Science 222, 616–618. <https://doi.org/10.1126/science.222.4624.616>
- 805 806 Whitmore, B.M., Ohman, M.D., 2021. Zooglider-measured association of zoo-  
807 plankton with the fine-scale vertical prey field. Limnology and Oceanography  
808 66, 3811–3827. <https://doi.org/10.1002/lno.11920>
- 809 810 Wood, S.N., 2017. Generalized additive models: an introduction with R, Second  
edition. ed, Texts in statistical science. CRC Press/Taylor & Francis Group,  
811 Boca Raton London New York.
- 812 Wood, S.N., 2001. mgcv: GAMs and Generalized Ridge Regression for R 1.
- 813 814 Zasko, D.N., Rusanov, I.I., 2005. Vertical Distribution of Radiolarians and  
Their Role in Epipelagic Communities of the East Pacific Rise and the Gulf  
815 of California. Biology Bulletin 32, 279–287. <https://doi.org/10.1007/s10525-005-0001-2>

816

005-0103-5

Table 1: Generalized Additive Model results for integrated total Rhizarian abundance in different regions of the water column.

<b>Model</b>	Term	edf	F	p-value
<b>All Rhizaria</b>	Salinity	2.0818	4.654	<0.001
<b>Epipelagic</b>				
$R^2_{adj} = 0.42$	DO	0.8272	0.945	0.0136
	Silica	3.1206	15.75	<0.001
	NO3	2.9970	6.268	<0.001
	Primary	1.8367	2.099	<0.001
	Productivity			
	Particle	0.9282	2.566	<0.001
Concentra-				
tion				
<b>All Rhizaria</b>	Silica	0.6847	0.431	0.073
<b>Upper</b>				
<b>Mesopelagic</b>				
$R^2_{adj} = 0.406$	Avg Mass	1.5426	0.923	0.045
	Flux			
	Particle	3.2957	20.89	<0.001
Concentra-				
tion				

<b>Model</b>	Term	edf	F	p-value
<b>All Rhizaria</b>	Avg Mass	1.6632	1.824	0.002
<b>Lower</b>	Flux			
<b>Mesopelagic</b>				
$R^2_{adj} = 0.603$	Particle	0.7694	0.662	0.027
	Concentra-			
	tion			

Table 2: Taxa-specific generalized additive models for different regions of the water column.

Model	Term	edf	F	p-value
<b>Acantharea</b>	Salinity	2.264	4.113	<0.001
<b>Epipelagic</b>				
R2adj=0.53	O2	2.579	6.712	<0.001
	Avg Mass	4.810	22.81	<0.001
	Flux			
	Bacteria	1.599	1.317	0.0117
	#/L			
	Particle	0.853	1.158	0.0087
	Concentra-			
	tion			
<b>Acantharea</b>	Avg C Flux	1.296	0.621	0.0439
<b>Upper</b>				
<b>Mesopelagic</b>				
R2adj=0.231	Avg N Flux	1.619	1.283	0.0026
	Particle	0.952	3.886	<0.001
	Concentra-			
	tion			

Model	Term	edf	F	p-value
<b>Acantharea</b>	Temperature	2.076	4.155	<0.001
<b>Lower</b>				
<b>Mesopelagic</b>				
R2adj=0.509	Avg N Flux	1.494	1.216	0.0113
	Primary	0.766	0.648	0.0253
	Productivity			
	Particle	2.037	10.03	<0.001
	Concentra-			
	tion			
<b>Aulacanthidae</b>	Salinity	0.792	0.757	0.0241
<b>Epipelagic</b>				
R2adj=0.251	Avg N Flux	0.869	1.324	0.0018
	Primary	2.312	7.704	<0.001
	Productivity			
	Particle	2.008	2.200	0.0017
	Concentra-			
	tion			
<b>Aulacanthidae</b>	Particle	2.832	9.802	<0.001
<b>Upper</b>	Concentra-			
<b>Mesopelagic</b>	tion			

Model	Term	edf	F	p-value
R2adj = 0.158				
<b>Aulacanthidae</b>	Avg Mass	1.622	1.991	0.002
<b>Lower</b>	Flux			
<b>Mesopelagic</b>				
R2adj=0.298	Particle	2.123	6.706	<0.001
	Concentra-			
	tion			
<b>Aulosphaeridae</b>	Particle	2.653	13.06	<0.001
<b>Upper</b>	Concentra-			
<b>Mesopelagic</b>	tion			
R2adj=0.2				
<b>Aulosphaeridae</b>	Particle	0.972	6.248	<0.001
<b>Lower</b>	Concentra-			
<b>Mesopelagic</b>	tion			
R2adj=.147				
<b>Castanellidae</b>	Avg C Flux	1.462	0.816	0.0421
<b>Epipelagic</b>				

Model	Term	edf	F	p-value
R2adj = 0.124	Primary	0.771	0.665	0.0247
	Productivity			
	Particle	3.956	4.623	<0.001
	Concentra-			
	tion			
<b>Coelodendridae</b>	Avg N Flux	0.822	0.919	0.0183
<b>Upper</b>				
<b>Mesopelagic</b>				
R2adj=.113	Particle	0.970	6.208	<0.001
	Concentra-			
	tion			
<b>Coelodendridae</b>	Particle	1.773	4.873	<0.001
<b>Lower</b>	Concentra-			
<b>Mesopelagic</b>	tion			
R2adj=.133				
<b>Collodaria</b>	Salinity	0.925	2.267	<0.001
<b>Epipelagic</b>				
R2adj=0.16	O2	2.015	2.217	0.002

Model	Term	edf	F	p-value
	Bacteria	1.843	2.100	0.002
	#/L			
<b>Foraminifera</b>	Temperature	4.414	8.789	<0.001
<b>Epipelagic</b>				
R2adj=0.445	O2	1.603	1.287	0.0111
	Avg N Flux	2.512	3.396	<0.001
	Primary	0.824	0.920	0.0153
	Productivity			
	Particle	0.919	2.257	<0.001
	Concentra-			
	tion			

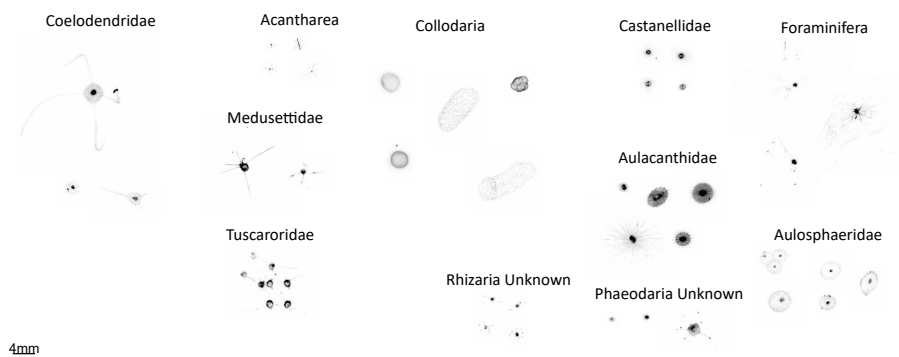


Figure 1: Example images of different Rhizaria taxa. 4mm scale bar shown in lower right. All vignettes are same scale

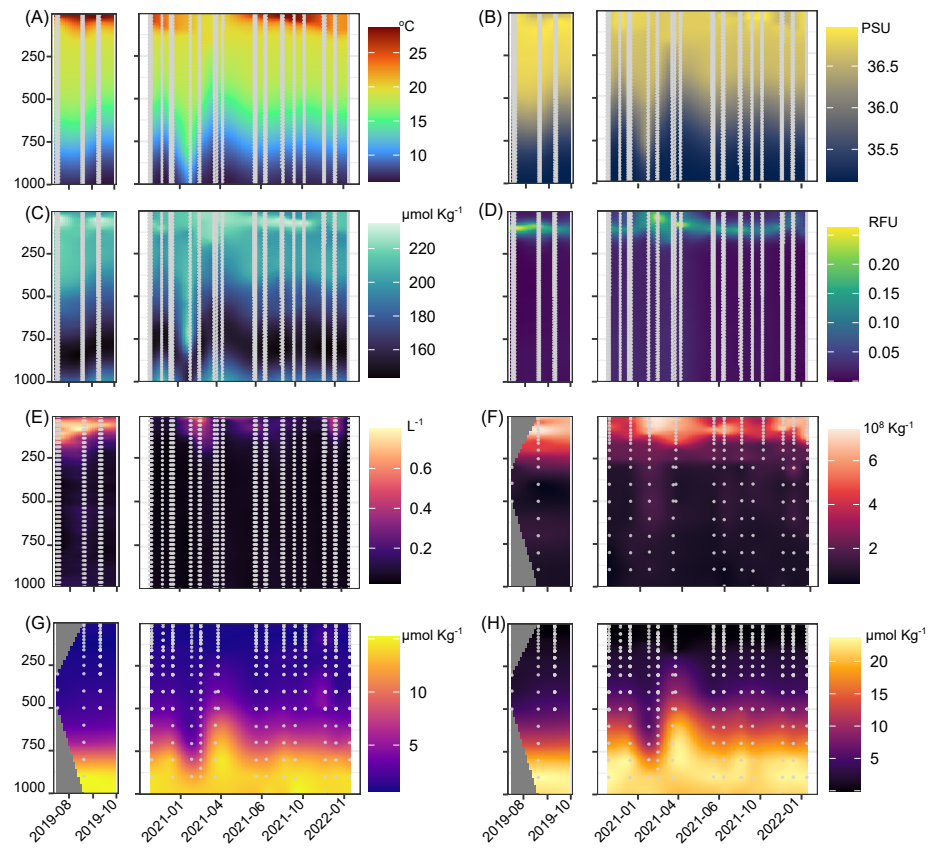


Figure 2: Environmental profiles across time-series of study period. Y axis shows depth in meters. (A) Temperature. (B) Salinity. (C) Dissolved Oxygen. (D) In-situ chlorophyll fluorescence. (E) Particle concentration ( $184 - 450 \mu\text{m}$ ). (F) Bacteria Abundance. (G) Silica. (H) Nitrate

817 end.

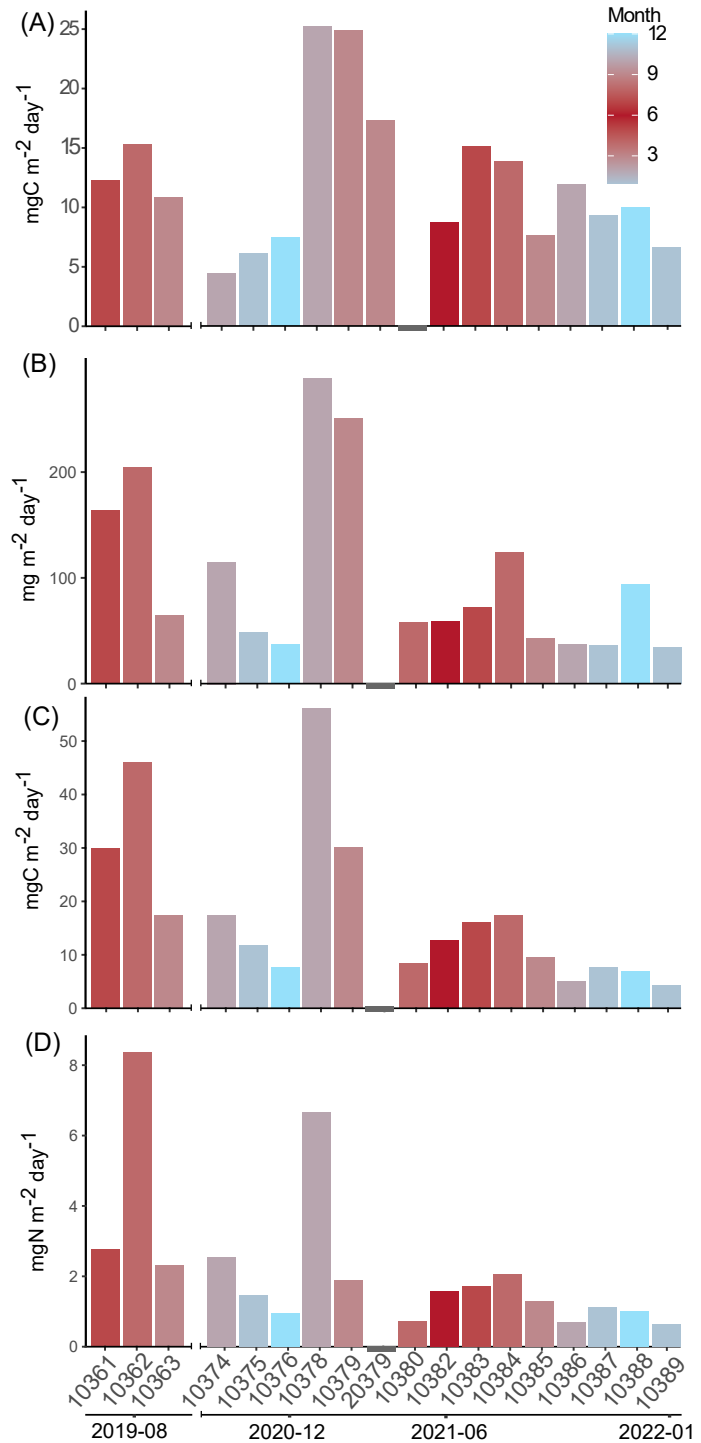


Figure 3: Primary productivity (A) and flux estimates from total mass (B), carbon (C), and nitrogen (D). Values are from monthly cruises with month displayed in corresponding colors. Absent data are shown by grey bar.

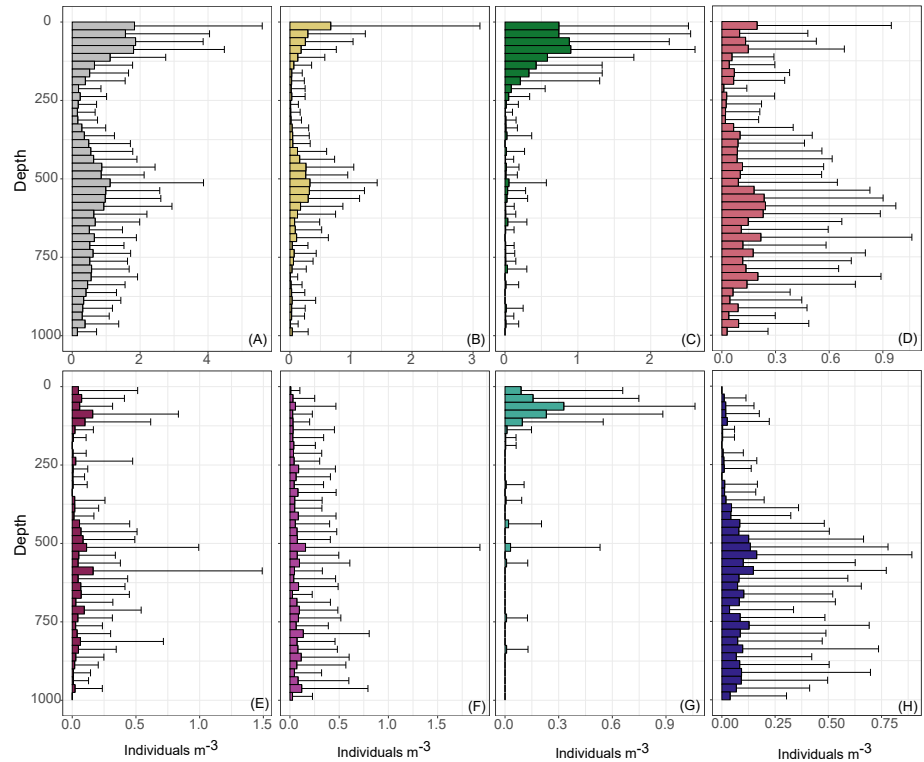


Figure 4: Average abundance of Rhizaria in 25m bins, across entire study period. Shown are total Rhizaria (A), Acantharea (B), Collodaria (C), Aulacanthidae (D), Foraminifera (E), Aulosphaeridae (F), Castanellidae (G), Coelodendridae (H).

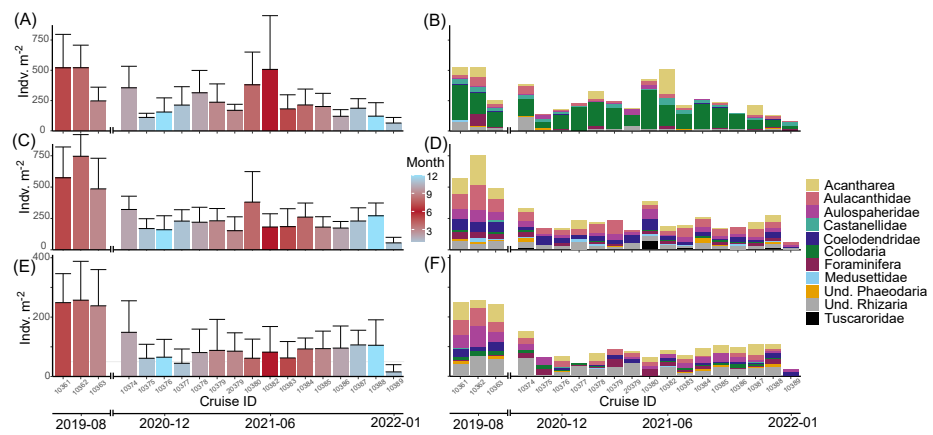


Figure 5: Seasonality of Rhizarian integrated abundance for the epipelagic (0-200m) (A-B), upper mesopelagic (200-500m) (C-D), lower mesopelagic (500-1000m) (E-F). Left panels (A,C,E) display total integrated abundance per monthly cruise colored by month. Right panels (B, D, F) display community composition of each total abundance.

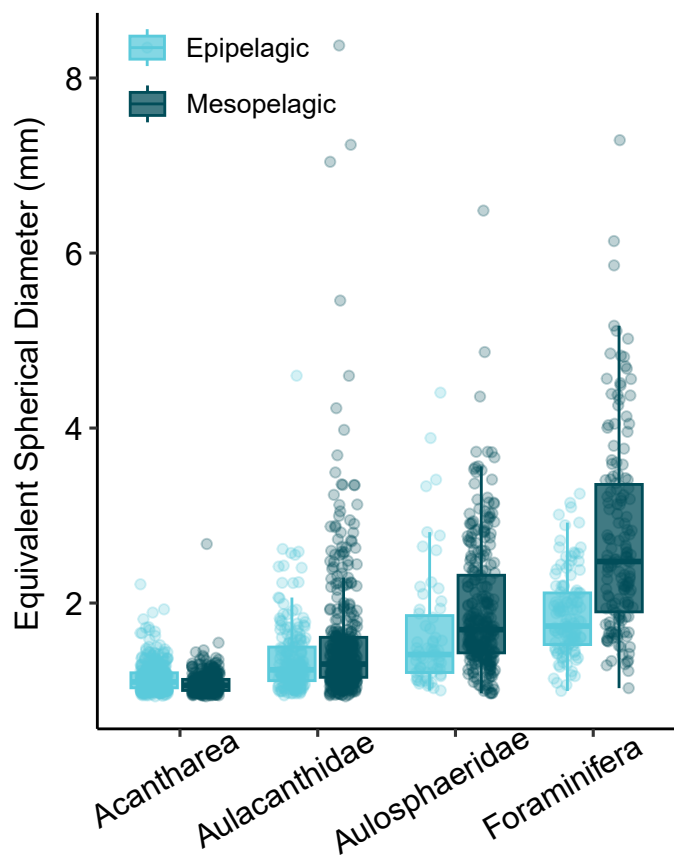


Figure 6: Comparison of average sizes (ESD) amongst Rhizarian taxa which occurred throughout the water column.

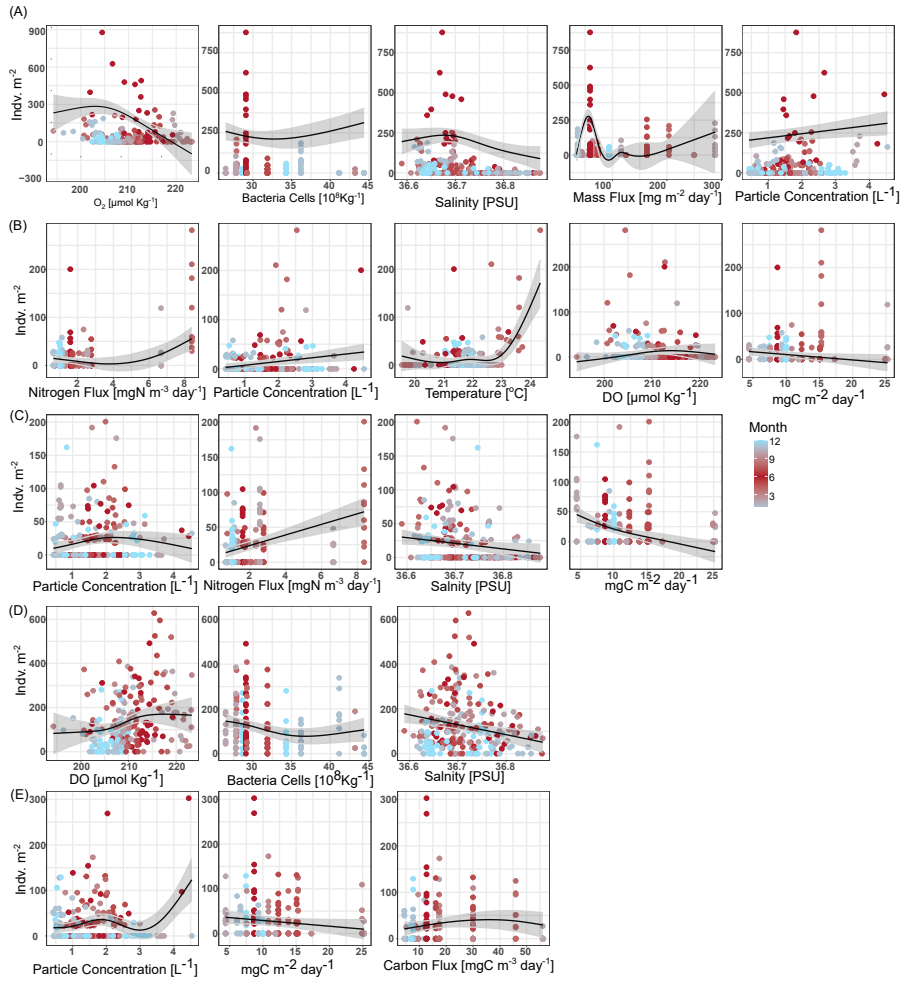


Figure 7: Partial effects of smooth terms in taxa-specific GAM models from the epipelagic (0-200m). Effects are grouped by taxa; Acantharea (A), Foraminifera (B), Aulacanthidae (C), Collodaria (D), Castanellidae (E).

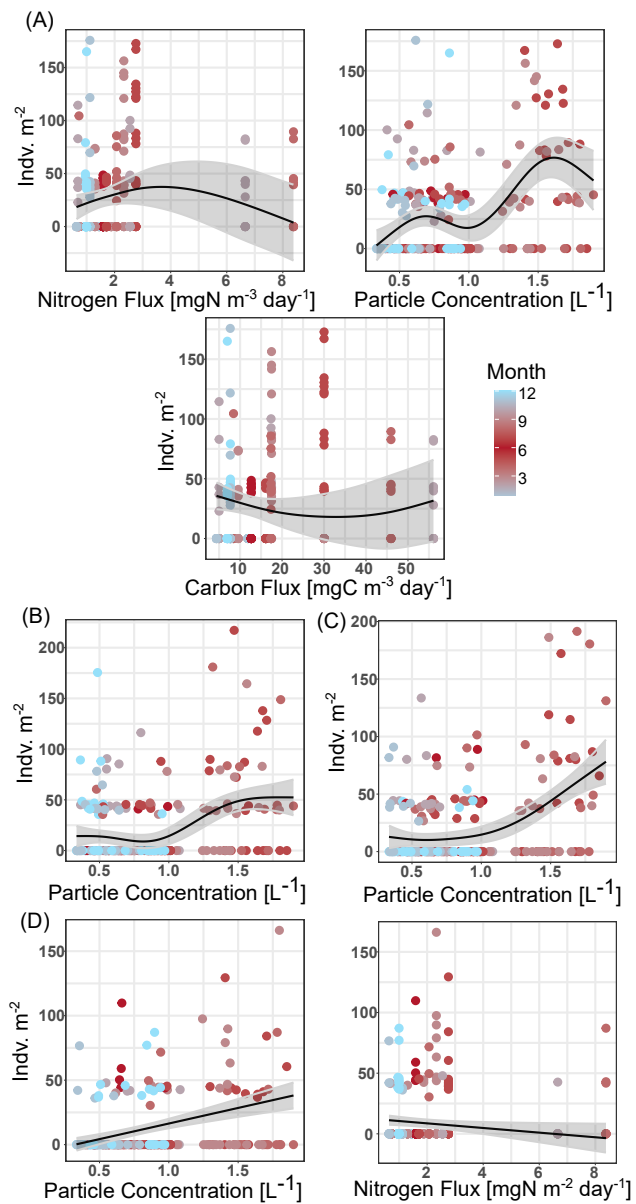


Figure 8: Partial effects of smooth terms in taxa-specific GAM models from the upper mesopelagic (200-500m). Effects are grouped by taxa; Acantharea (A), Aulacanthidae (B), Aulosphaeridae (C), Coelodendridae (D).

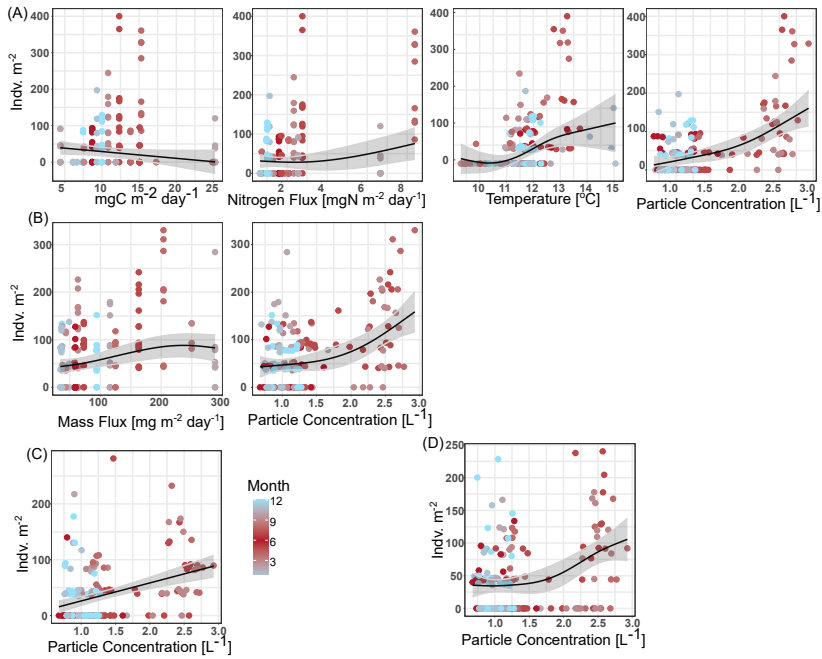


Figure 9: Partial effects of smooth terms in taxa-specific GAM models from the lower mesopelagic (500-1000m). Effects are grouped by taxa; Acantharea (A), Aulacanthidae (B), Aulosphaeridae (C), Coelodendriidae (D).